3. Singh, U. C.; Kollman, P. A. *J. Comp. Chem.* **1984**, *5*, 129.
4. Lavery, R.; Zakrzewska, K.; Pullman, A. *J. Comp. Chem.* **1984**, *5*, 363.
5. Houser, J. J.; Klopman, G. *J. Comp. Chem.* **1988**, *9*, 893.
6. (a) Mulliken, R. S. *J. Chem. Phys.* **1955**, *23*, 1833. (b) *ibid*, **1955**, *23*, 1841.
7. Momany, F. A. *J. Phys. Chem.* **1978**, *82*, 592.
8. Cox, S. R.; Williams, D. E. *J. Comp. Chem.* **1981**, *2*, 304.
9. Sanderson, R. T. *Chemical Bonds and Bond Energy*; Academic Press: New York, 1976; p 15.
10. Gasteiger, J.; Marsili, M. *Tetrahedron* **1980**, *36*, 3219.
11. Mortier, W. J.; Genechten, K. W.; Gasteiger, J. *J. Am. Chem. Soc.* **1985**, *107*, 829.
12. (a) No, K. T.; Grant, J. A.; Scheraga, H. A. *J. Phys. Chem.* **1990**, *94*, 4732. (b) No, K. T.; Grant, J. A.; Jhon, M. S.; Scheraga, H. A. *J. Phys. Chem.* **1990**, *94*, 4740. (c) Park, J. M.; No, K. T.; Jhon, M. S.; Scheraga, H. A. *J. Comp. Chem.* **1993**, *14*, 1482. (d) Park, J. M.; Kwon, O. Y.; No. K. T.; Jhon, M. S.; Scheraga, H. A. *J. Comp. Chem.* **1995**, *16*, 1011.
13. (a) Abraham, R.; Grant, G. H. *J. Comp. Chem.* **1988**, *9*, 244. (b) *ibid*, **1988**, *9*, 709.
14. Cohen de Lara, E.; Tan T. N. *J. Phys. Chem.* **1976**, *80*, 1917.
15. Mortier, W. J. *J. Catal.* **1978**, *55*, 138. (b) No, K. T.; Grant, J. A.; Jhon, M. S.; Scheraga, H. A. *J. Phys. Chem.* **1990**, *94*, 4740.
16. (a) No, K. T.; Jhon, M. S. *J. Kor. Chem. Soc.* **1979**, *23*, 374. (b) No, K. T.; Chon, H.; Ree, T.; Jhon, M. S. *J. Phys. Chem.* **1981**, *85*, 2065. (c) No, K. T.; Kim, J. S.; Huh, Y. Y.; Kim, W. K.; Jhon, M. S. *J. Phys. Chem.* **1987**, *91*, 740. (d) No, K. T.; Huh, Y. Y.; Jhon, M. S. *J. Phys. Chem.* **1989**, *93*, 6413.
17. Huheey, E. *J. Phys. Chem.* **1965**, *69*, 3284.
18. Frisch, M. J.; Head-Gordon, M.; Foresman, J. B.; Trucks, G. W.; Raghavachari, K.; Schlegel, H. B.; Robb, M. A.; Binkley, J. S.; Gonzalez, C.; Defrees, D. J.; Fox, D. J.; Whiteside, R. A.; Seeger, R.; Melius, C. F.; Baker, J.; Kahn, L. R.; Stewart, J. J. P.; Fluder, E. M.; Topiol, S.; Pople, J. A. *Gaussian 90*; Gaussian Inc., Pittsburgh, 1992.

Remarkable Structure Relaxation of Zeolite Windows in Rb_3- and K_3-A Crystal Structures of $M_3Na_{9-x}H_xSi_{12}Al_{12}O_{48}$, where M=Rb or K and x=1 or 0

Chong Sam Park, Myoung Sook Yoon, Woo Taik Lim, Myoung Chul Kim†, Soong Hyuck Suh‡, and Nam Ho Heo*

Department of Industrial Chemistry, Kyungpook National University, Taegu 702-701, Korea
†College of General Education, Kyungpook Sanup University, Taegu 701-702, Korea
‡Department of Chemical Engineering, Keimyung University, Taegu 704-701, Korea
Received May 16, 1995

Four crystal structures of M_3-A ($M_3Na_{9-x}H_x$-A, M=Rb or K and x=1 or 0), Rb_3Na_8H-A (a=12.228(1) Å and R_1=0.046), Rb_3Na_9-A (a=12.258(3) Å and R_1=0.058), K_3Na_8H-A (a=12.257(3) Å and R_1=0.048) and K_3Na_9-A (a=12.257(3) Å and R_1=0.052), have been determined by single crystal x-ray diffraction technique in the cubic space group $Pm\bar{3}m$ at 21 ℃. In all structures, each unit cell contained three M^+ ions all located at one crystallographically distinct position on 8-rings. Rb^+ ions are 3.12 and 3.21 Å away respectively from O(1) and O(2) oxygens, about 0.40 Å away from the centers of the 8-rings, and K^+ ions are 2.87 and 2.81 Å apart from the corresponding oxygens. These distances are the shortest ones among those previously found for the corresoponding ones. Eight 6-rings per unit cell are occupied by eight Na^+ ions, each with a distance of 2.31 Å to three O(3) oxygens. The twelfth cation per unit cell is found as Na^+ opposite 4-ring in the large cavities of M_3Na_9-A and assumed to be H^+ for M_3Na_8H-A. With these noble non-framework cationic arrangements, larger M^+ ions preferably on all larger 8-rings and the compact Na^+ ions on all 6-rings, the bond angles in the 8-rings of M_3-A, 145.1 and 161.0 respectively for (Si,Al)-O(1)-(Si,Al) and (Si,Al)-O(2)-(Si,Al), turned out to be remarkably stable and smaller, by more than 12 to 17°, than the corresponding angles found in the crystal structures of zeolites A with high concentration of M^+ ions. It is to achieve these remarkably relaxed 8-rings, the main windows for the passage of gas molecules, with simultaneously maximized cavity volumes that M_3-A have been selected as one of the efficient zeolite A systems for gas encapsulation.

Introduction

Large quantities of gas molecules, having kinetic diameters somewhat larger than those of zeolite windows, can be encapsulated in the molecular-dimensioned cavities of zeolite by heating the zeolite and subsequent quenching to ambient temperature while the high pressure is maintained.[1~5] These encapsulated gas molecules in the zeolitic cavities can sustain high-pressure concentrations without leakage even at room temperature. The utilization of zeolites as such storage med-

ium for small gas molecules was suggested long ago by G. A. Cook,[6] D. W. Breck,[1] and R. M. Barrer *et al.*[7~10] from their extensive experimental and theoretical studies of the encapsulation phenomena.

In case of zeolite A, it is known that both types of cavities (α- and β- cages or large cavity and sodalite unit) can be utilized as microcontainers of small gas molecules, when the gas molecules are encapsulated into zeolite A with all 8-oxygen-ring (8-ring) windows blocked by large monopositive cations such as Cs^+, Rb^+, or K^+.[11~17] In order to maximize the encapsulation capacity of the zeolites A, each unit cell of zeolite A should contain a certain number of such large cations (2.3 to 3.0 per $Pm\bar{3}m$ unit cell) which must all be located on main windows (8-rings), leaving the cavities relatively undamaged for maximum volume.[11,14,16,17] It has also been known that any extra of such large cations located in deep cavities of zeolite A results in reducing the diffusion rate of en- and decapsulating gas molecules through channels of the cavities.[18,19] Therefore, it seems that the composition of the most effective zeolite A for the gas storage system should be somewhat like M_xNa_{12-x}-A ($M_xNa_{12-x}Si_{12}Al_{12}O_{48}$),[20] where M=Cs, Rb, or K and $2.3 \le x \le 3.0$ (M_3-A). However, the actual positions of such large cations within M_3-A remained unknown, except for those of Cs_3-A reported previously,[21,22] and only a little about the geometry around them on the main windows could be deduced from the known crystal structures of zeolites A, fully or near fully ion-exchanged with M^+ ions.

In the crystal structures of $Rb_{11}Na$-A and K_{12}-A,[23,24] such large cations are found on 8-ring-windows as well as opposite 6-rings in deep sodalite unit and large cavity. In order to accommodate large number of such cations from the inner surfaces of the cavities, the geometry around oxide anions of 6- and 8-rings had to be severely distorted, modifying the apertures and shapes of the cavities and resulting in somewhat unusual geometry of framework with probably different sorption and encapsulation properties. For example, considering the size of Rb^+ ion (r_{Rb^+}=1.47 Å) which is in between those of Cs^+ (r_{Cs^+}=1.67 Å) and K^+ (r_{K^+}=1.33 Å) ions,[25,26] the most probable site of Rb^+ ion on the 8-ring would be the vicinity of its center within the coordination spheres of framework oxide anions, rather than the center at which Rb^+ ion was found experimentally in $Rb_{11}Na$-A.[23] This rather unreasonable locations of Rb^+ ions at the centers of 8-rings in $Rb_{11}Na$-A would have not been possible, unless there have been such severe distortion of framework with such high concentration of Rb^+ ions. In M_3-A, however, the detailed structures of 8-rings, the principal windows for the passage of gas molecules,[27] should be different and probably far less distorted due to the complete absence of the large cations deep in the cavities.

Keeping those experimental evidences of the gas encapsulation in mind as well as others of above structural considerations, knowledge on the exact positions of the cations and geometry around the main windows (8-rings) of those zeolites A must play an important role in understanding the gas encapsulation phenomena. Therefore, a detailed crystallographic study on those partially M^+-exchanged zeolites A (M_3-A) will have important consequences in developing such gas storage medium of zeolites. In this work, zeolites A with the compositions of M_3-A, where M=Rb and K, have been prepared and their crystal structures were studied crystallographically. Together with those of Cs_3-A reported earlier,[21,22] various changes in the geometry around M^+ ions and framework atoms, hence changes in the pore-opening and shapes of zeolitic cavities, were thoroughly examined.

Experimental

Colorless crystals of Na_{12}-A·$27H_2O$[20] were synthesized by Charnell's method.[28] Single crystals of Rb_3Na_8H-A (crystal 1) and Rb_3Na_9-A (crystal 2) have been prepared by using dynamic ion-exchange method (flowing stream) with aqueous solutions, 0.06 in Na^+ and 0.04 M in Rb^+, of nitrates (pH= 6.0 with $NaNO_3$, 99.99%, and $RbNO_3$, 99.7%) for crystal 1 and of hydoxides (pH=13.3 with NaOH, 99.99%, and RbOH, 99.9%) for crystal 2. Ion exchange of K^+ was similarly performed with aqueous solutions, 0.09 in Na^+ and 0.01 M in K^+, made by using nitrates (the $NaNO_3$ and KNO_3, 99.995%, pH=6.8) for K_3Na_8H-A (crystal 3) and by using hydroxides (the NaOH and KOH·H_2O, 99.99%, pH=11.7) for Rb_3Na_9-A (crystal 4). All reagents were purchased from Aldrich Chem. Co. These solution compositions were chosen so that all 8-ring sites would be occupied by Rb^+ and K^+ ions, respectively for Rb_3-A and K_3-A.[15]

Each single crystal of above hydrated M_3-A, a cube 80 μm on an edge, was lodged in a fine Pyrex capillary on a vacuum line. After cautious increases in temperature of 25 ℃/h and following complete dehydration at 350 ℃ and 5×10^{-6} Torr for four days, the crystal-containing capillary still under vacuum was sealed off from the vacuum line at room temperature for x-ray experiments. No changes were noted in the appearance of the crystals upon examination under the microscope.

The cubic space group $Pm\bar{3}m$ (no systematic absences) was used for the crystallographic studies of this work with reasons discussed previously.[29,30] A CAD4/Turbo diffractometer equipped with a rotating anode generator and a graphite monochromator was used for preliminary experiments and for the subsequent collection of diffraction intensities, all at 21(1) ℃. Molybdenum radiation ($K\alpha_1$, λ=0.70930 Å; $K\alpha_2$, λ= 0.71359 Å) was used. In each case, the cell constant, a= 12.228(1), 12.258(3), 12.257(3), and 12.257(3) Å for crystals 1 to 4, respectively, was determined by a least-squares treatment of 15 intense reflections for which $20<2\theta<30°$. Experimental details including the diffraction intensity collection and data reduction are same as previously presented.[21,22] Absorption corrections (μR *ca.* 0.25, 0.25, 0.14, and 0.15 for crystals 1 to 4,[31] respectively) were judged to be negligible for all crystals. Only those reflections in each final data set ($2\theta<$ 70°) for which the net count exceeded three times its standard deviation were used in structure solution and refinement. This amounted to 161, 171, 206, and 211 reflections for crystals 1 to 4, respectively.

Structure Determination

Rb_3Na_8H-A (crystal 1) and Rb_3Na_9-A (crystal 2). Full-matrix least-squares refinement[32] for crystal 1 was initiated with the atomic parameters of framework atoms [(Si, Al), O(1), O(2), and O(3)], and Na^+ at Na in Cs_3Na_8H-A.[21,22] The refinement with isotropic parameter for the Na converged

to error indices of $R_1=\Sigma||F_o|-|F_c||/\Sigma F_o=0.243$ and $R_2=(\Sigma w(F_o-|F_c|)^2/\Sigma wF_o^2)^{1/2}=0.325$. Introducing Rb^+ ions at a peak (0, 1/2, 1/2, at the centers of 8-rings) found in a difference Fourier function caused quick convergence to $R_1=0.072$ and $R_2=0.076$ with large thermal parameter for Rb^+ ions, suggesting that these Rb^+ are located somewhat away from the centers. When the point symmetry of Rb^+ ions at Rb lowered (from 0, 1/2, 1/2 to 0, z, z) in following least-squares refinement, they were stable at (0, 0.4767, 0.4767) with remarkable lowering of error indices (about 1%), R_1 to 0.063 and R_2 to 0.066, and resulting occupancies of 2.98(3) and 8.34(10) for Rb and Na, respectively. Extensive but unsuccessful efforts were made to locate the twelfth cation necessary for electroneutrality at the usual position opposite a 4-ring in the large cavity. The final cycles of refinement with anisotropic thermal parameters for all atoms and a fixed occupancy of 3.0 and 8.0 (their maximum values by symmetry) respectively for Rb and Na converged to the error indices $R_1=0.046$ and $R_2=0.047$. Considering the moderate amount of H^+ in the ion-exchange solution (pH=6.0), and the small deviation from unity which may be expected for Si/Al (perhaps 1.04),[33] the unit cell formula of this crystal is taken to be $Rb_3Na_8H_x$-A, *x ca.* 1.[20] For simplicity, the notation Rb_3Na_8H-A will be used.

Similar refinement procedures were carried out for crystal 2, except for the successful location of an additional Na^+ at Na(2). When a peak at (0.210, 0.210, 1/2) found in difference Fourier function was introduced as the twelfth Na^+ ion at Na(2) in the refinement, it was stable and converged at the usual position, opposite 4-ring, with error indices of $R_1=0.056$ and $R_2=0.055$ and resulting occupancies of 2.79(3), 8.4(1), and 1.1(2), respectively for Rb, Na, and Na(2). Final cycles of refinement with occupancies fixed at 3.0, 8.0, and 1.0 for Rb, Na, and Na(2), respecitvely, converged to the

Table 1. Positional, Thermal, and Occupancy Parameters of Dehydrated M_3-A Zeolites[a]

	Wyckoff Position	*x*	*y*	*z*	β_{11}[b] or B_{iso}[c]	β_{22}	β_{33}	β_{12}	β_{13}	β_{23}	Occupancy[d] fixed	Occupancy[d] varied
					(a) Rb_3Na_8H-A, crystal 1							
(Si,Al)	24(*k*)	0	1837(2)	3715(2)	28(2)	27(2)	13(2)	0	0	7(4)	24[e]	
O(1)	12(*h*)	0	2240(8)	5000[f]	47(9)	73(10)	15(7)	0	0	0	12	
O(2)	12(*i*)	0	2942(6)	2942(6)	96(11)	33(5)	33(5)	0	0	40(15)	12	
O(3)	24(*m*)	1126(4)	1126(4)	3398(5)	48(3)	48(3)	52(6)	28(11)	−5(9)	−5(9)	24	
Na	8(*g*)	2033(5)	2033(5)	2033(5)	78(3)	78(3)	78(3)	116(7)	116(7)	116(7)	8	8.3(1)
Rb	12(*i*)	0	4771(4)	4771(4)	122(7)	101(6)	101(6)	0	0	−49(19)	3	2.98(3)
					(b) Rb_3Na_9-A, crystal 2							
(Si,Al)	24(*k*)	0	1835(3)	3719(3)	30(2)	19(2)	10(2)	0	0	7(5)	24[e]	
O(1)	12(*h*)	0	2250(10)	5000[f]	30(10)	48(11)	28(10)	0	0	0	12	
O(2)	12(*i*)	0	2920(7)	2920(7)	71(12)	33(6)	33(6)	0	0	29(19)	12	
O(3)	24(*m*)	1125(4)	1125(4)	3424(7)	36(4)	36(4)	42(7)	11(13)	4(9)	4(9)	24	
Na	8(*g*)	2019(5)	2019(5)	2019(5)	53(4)	53(4)	53(4)	60(9)	60(9)	60(9)	8	8.4(1)
Rb	12(*i*)	0	4798(7)	4798(7)	118(9)	141(8)	141(8)	0	0	−51(47)	3	2.79(3)
Na(2)	12(*j*)	2457(87)	2457(87)	5000[f]	9(5)						1	1.1(2)
					(c) K_3Na_8H-A, crystal 3							
(Si,Al)	24(*k*)	0	1834(2)	3714(2)	28(1)	27(1)	16(1)	0	0	8(3)	24[e]	
O(1)	12(*h*)	0	2293(6)	5000[f]	53(7)	60(7)	33(6)	0	0	0	12	
O(2)	12(*i*)	0	2923(4)	2923(4)	75(7)	36(4)	36(4)	0	0	39(10)	12	
O(3)	24(*m*)	1123(4)	1123(3)	3406(4)	49(3)	49(3)	45(4)	12(8)	2(6)	2(6)	24	
Na	8(*g*)	2025(3)	2025(3)	2025(3)	68(2)	68(2)	68(2)	57(5)	57(5)	57(5)	8	7.8(1)
K	12(*i*)	0	4531(8)	4531(8)	191(21)	150(14)	150(14)	0	0	−61(26)	3	3.07(5)
					(d) K_3Na_9-A, crystal 4							
(Si,Al)	24(*k*)	0	1835(2)	3719(2)	24(1)	25(1)	15(1)	0	0	12(3)	24[e]	
O(1)	12(*h*)	0	2260(7)	5000[f]	39(6)	65(7)	19(6)	0	0	0	12	
O(2)	12(*i*)	0	2931(5)	2931(5)	65(8)	36(4)	36(4)	0	0	29(11)	12	
O(3)	24(*m*)	1123(3)	1123(3)	3422(4)	47(3)	47(3)	32(4)	8(9)	5(5)	5(5)	24	
Na	8(*g*)	2008(3)	2008(3)	2008(3)	64(3)	64(3)	64(3)	43(6)	43(6)	43(6)	8	7.8(1)
K	12(*i*)	0	4556(8)	4556(8)	126(16)	139(13)	139(13)	0	0	−57(26)	3	2.83(5)
Na(2)	12(*j*)	2315(54)	2315(54)	5000[f]	8(3)						1	0.7(1)

[a] Positional and anisotropic thermal parameters are given $\times 10^4$. Numbers in parentheses are the estimated standard deviations in the units of the least significant figure given for the corresponding parameter. The anisotropic temperature factor is $\exp[-(\beta_{11}h^2+\beta_{22}k^2+\beta_{33}l^2+\beta_{12}hk+\beta_{13}hl+\beta_{23}kl)]$. [b] R. m. s. displacements can be calculated from β_{ii} values using formula $\mu_i=0.225a(\beta_{ii})^{1/2}$, where $a=12.260$ Å. [c] Isotropic thermal parameter in units of Å^2. [d] Occupancy factors are given as the number of atoms or ions per unit cell. [e] Occupancy for (Si)=12, occupancy for (Al)=12. [f] Exactly 1/2 by symmetry.

Table 2. Selected Interatomic Distances (Å) and Angles (deg)[a]

Bond and Angle	Rb_3Na_8H-A (crystal 1)	Rb_3Na_9-A (crystal 2)	K_3Na_8H-A (crystal 3)	K_3Na_9-A (crystal 4)
(Si,Al)-O(1)	1.648(5)	1.651(6)	1.652(4)	1.654(4)
(Si,Al)-O(2)	1.649(8)	1.652(10)	1.650(6)	1.654(6)
(Si,Al)-O(3)	1.673(5)	1.671(6)	1.672(4)	1.670(5)
Na-O(3)	2.291(8)	2.316(9)	2.304(6)	2.315(6)
Na-O(2)	2.941(4)	2.926(8)	2.930(5)	2.936(5)
Rb-O(1)	3.11(3)	3.13(6)	–	–
Rb-O(2)	3.16(2)	3.26(4)	–	–
K-O(1)	–	–	2.87(2)	2.87(1)
K-O(2)	–	–	2.79(1)	2.82(1)
Na(2)-O(1)		3.02(1)	–	2.84(8)
Na(2)-O(3)	–	3.01(7)	–	2.83(4)
O(1)-(Si,Al)-O(2)	107.5(5)	108.4(6)	108.5(4)	107.4(4)
O(1)-(Si,Al)-O(3)	112.1(3)	111.5(4)	111.8(3)	112.4(3)
O(2)-(Si,Al)-O(3)	107.1(2)	106.9(3)	106.8(2)	107.3(2)
O(3)-(Si,Al)-O(3)	110.7(4)	112.0(3)	110.8(3)	111.9(2)
(Si,Al)-O(1)-(Si,Al)	145.1(8)	144(1)	145.0(6)	143.3(7)
(Si,Al)-O(2)-(Si,Al)	159.9(5)	162.8(7)	162.0(4)	161.5(4)
(Si,Al)-O(3)-(Si,Al)	143.3(5)	144.4(5)	143.8(4)	143.8(1)
O(3)-Na-O(3)	118.2(3)	118.7(3)	118.3(2)	118.8(2)

[a]The numbers in parentheses are the estimated standard deviations in the units of the least significant digit given for the corresponding parameters.

error indices $R_1=0.058$ and $R_2=0.061$, resulting the formula of Rb_3Na_9-A for this crystal. Final difference Fourier functions were featureless for both crystals. The final structural parameters are given in Table 1(a) and 1(b) and selected interatomic distances and angles are given in Table 2, respectively.

K_3Na_8H-A (crystal 3) and K_3Na_9-A (crystal 4). Full-matrix least-squares refinement for crystal 3 began with the atomic parameters of framework atoms and Na^+ ions at Na on 6-rings in Cs_3Na_8H-A.[21,22] Introducing an additional peak at K (0, 0.46,0.46) found in subsequent difference Fourier function caused convergence to $R_1=0.047$ and $R_2=0.045$ with resulting occupancies of 3.07(5) and 7.82(10) for Rb and Na, respectively. Similar unsucessful efforts were made in locating the twelfth cation. Final cycles of refinement with occupancies fixed at 3.0 and 8.0 for Rb and Na, respectively, converged to the error indices $R_1=0.048$ and $R_2=0.046$. With the reasons described in crystal 1, the notation K_3Na_8H-A will be used for this crystal. The refinements for the crystal 4 were similarly carried out, except for the twelfth Na^+ ion at Na(2). Refinement including Na(2) at (0.21, 0.21, 0.5) with an isotropic thermal parameter lowered the error indices to $R_1=0.052$ and $R_2=0.047$, resulting occupancies of 2.83(5), 7.82(10), and 0.72(10) for K, Na, and Na(2), respectively. Final cycles of refinement with occupancies fixed at 3.0 and 8.0 for K and Na, respecitvely, converged to the error indices $R_1=0.052$ and $R_2=0.048$, confirming the formula of K_3Na_9-A for this crystal. The final structural parameters are given in Table I(c) and I(d) and the selected interatomic distances and angles are given in Table 2, respectively.

The values of the goodness-of-fit, $(\Sigma w(F_o-|F_c|)^2/(m-s))^{1/2}$, are 1.50, 1.79, 1.27, and 1.36; the number of observations, m, are 161, 171, 206, and 211, and the number of parameters, s, are 28, 30, 28, and 30 for crystals 1 to 4, respectively. All shifts in the final cycles of refinement for both crystals were less than 0.1% of their corresponding estimated standard deviations. The quantity minimized in least-squares is $\Sigma w(F_o-|F_c|)^2$, and the weights (w) are the reciprocal squares of $\sigma(F_o)$, the standard deviation of each observed structure factor. Atomic structure factors for Rb^+, K^+, Na^+, O^-, and $(Si, Al)^{1.75+}$ were used.[34,35] The function describing $(Si, Al)^{1.75+}$ is the mean of the Si^{4+}, Si^0, Al^{3+}, and Al^0 functions. All scattering factors were modified to account for anomalous dispersion.[36,37]

Discussion

In all four crystal structures of fully dehydrated $M_3Na_{9-x}H_x$-A, M=Rb or K and $x=1$ or 0 (crystals 1 to 4), each unit cell contained three Rb^+ or K^+ ions all located at one crystallographically distinct position, Wycoff position of 12(*i*) with point symmetry of *mm*, on the 8-rings. Eight 6-rings per unit cell are fully occupied by eight Na^+ ions as those seen in the crystal structure of Na_{12}-A.[38] The twelfth cation per unit cell, necessary for electroneutrality of framework, is found as Na^+ opposite 4-ring in the large cavities of M_3Na_9-A (crystals 2 and 4). In cases of M_3Na_8H-A (crystals 1 and 3), each unit cell is assumed to contain H^+ ion as the twelfth cation by reasons described above and confirmed previously in Cs_3Na_8H-A.[21,22]

Rb_3-A ($Rb_3Na_{9-x}H_x$-A, $x=1$ or 0). In both structures of Rb_3Na_8H-A and Rb_3Na_9-A (crystals 1 and 2), three Rb^+ ions per unit cell fill the three 8-rings. These Rb^+ ions are about 0.40 Å away from the centers of the 8-rings, at which Rb^+ ions are found in the crystal structure of $Rb_{11}Na$-A.[23] Each Rb^+ ion is 3.11(3) Å from four O(1) oxygens and 3.16 (2) Å from four O(2) oxygens in Rb_3Na_8H-A and is 3.13(6) and 3.26(4) for the corresponding bonds in Rb_3Na_9-A (see interatomic distances in Table 2). Although these distances are somewhat longer than the sum, 2.79 Å, of the conventional ionic radii of Rb^+ and O^{2-},[25,26] these positions are better defined by the results of crystallographic refinements (see structure determination) and by shorter Rb-O distances than those found in $Rb_{11}Na$-A (3.18(1) and 3.69(1) Å, respectively for Rb-O(1) and Rb-O(2)).[23] Especially, the bond distance of Rb-O(2) is much better defined by more than 0.5 Å, compared to the corresponding bond distance in $Rb_{11}Na$-A.

Eight Na^+ ions per unit cell are located near the centers of the eight 6-rings per unit cell. Each Na^+ ion is 2.291(8) Å from three O(3) oxygens in Rb_3Na_8H-A and 2.316(9) from three O(3) oxygens in Rb_3Na_9-A (see Table 2). These Na^+ ions extend 0.32 and 0.27 Å, respectively, into the large cavity from the (111) planes of O(3) (see Table 3). The O(3)-Na-O(3) angles are very close to 120° (118.2(3) and 118.7(3), respectively for crystals 1 and 2), showing that Na^+ ion is nearly trigonal with no strong ligational molecules in its primary coordination sphere. This proves that the complete dehydration is achieved in these crystals. In Rb_3Na_8H-A, the twelfth cation per unit cell, because it could not be located crystallographically, is assumed to be, at least predominantly, a H^+ ion. It is Na^+ or another alkali metal cation in zeolite A ion-exchanged with alkali metal vapor[39] or with a basic

Table 3. Distances (Å) of Na from (111) Planes of O(3)

Rb_3Na_8H-A, crystal 1	0.32
Rb_3Na_9-A, crystal 2	0.27
K_3Na_8H-A, crystal 3	0.30
K_3Na_9-A, crystal 4	0.25

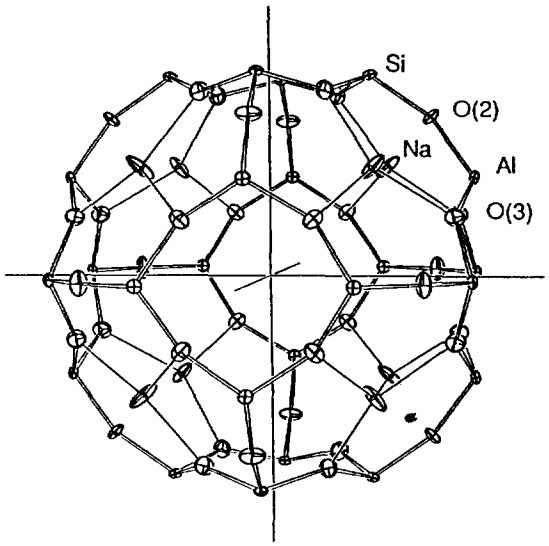

Figure 1. Sodalite unit of Rb_3Na_8H-A. The zeolite A framework is drawn with light bonds between tetrahedrally coordinated (Si, Al) and oxygen atoms. The bonds between the Na^+ ions and framework oxygens are indicated by fine solid lines. Ellipsoids of 20% probability are shown.

solution of an alkali metal salt. Indeed, about one Na^+ per unit cell was found opposite a 4-ring in the large cavity in Rb_3Na_9-A which was prepared by using the basic ion-exchange solution of hydroxide. This Na^+ ion is 3.02 Å away from O(1) and O(3) oxygens of the 4-ring and relatively longer than other Na-O distances because of averaging effect with low occupancy at this position. Otherwise, both crystal structures of Rb_3-A are crystallographically identical. Sodalite unit and large cavity of Rb_3Na_8H-A are shown in Figures 1 and 2, respectively.

K_3-A ($K_3Na_{9-x}H_x$-A, $x=1$ or 0). Three K^+ ions per unit cell of K_3Na_8H-A and K_3Na_9-A (crystals 3 and 4) are located on the 8-rings at the similar positions of those found in K_{12}-A.[24] Each K^+ ion is 2.87(2) and 2.79(1) Å from four O(1) and four O(2) oxygens, respectively, in K_3Na_8H-A and 2.87(1) and 2.82(1) Å for the corresponding bonds in K_3Na_9-A. Among the two kinds of approaches of K^+ ions to framework oxides of the 8-rings (O(1)'s and O(2)'s), the approach distances to O(1)'s, 2.87 Å in both structures, are somewhat similar with those in K_{12}-A, 2.86(3), while those to O(2)'s, 2.79(1) and 2.82(1) Å respectively for crystals 3 and 4, are remarkably shorter than those found in K_{12}-A, 3.37(5) Å.

Furthermore, the bond distances of K-O(2) in both K_3-A are somewhat shorter than those of K-O(1) with about 0.06 Å, 2.87-2.81 Å, of difference, while those of K-O(2) are much longer than those of K-O(1) by more than 0.51 Å, 3.37-2.86 Å, in K_{12}-A. This indicates that the electrons of O(1) and

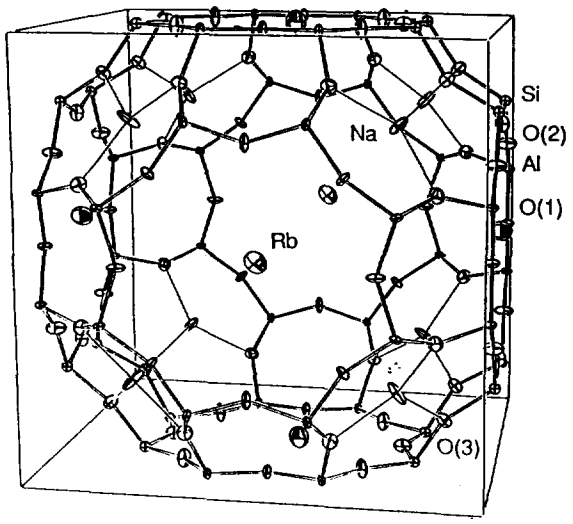

Figure 2. Large cavity of Rb_3Na_8H-A. See the caption to Figure 1 for other details.

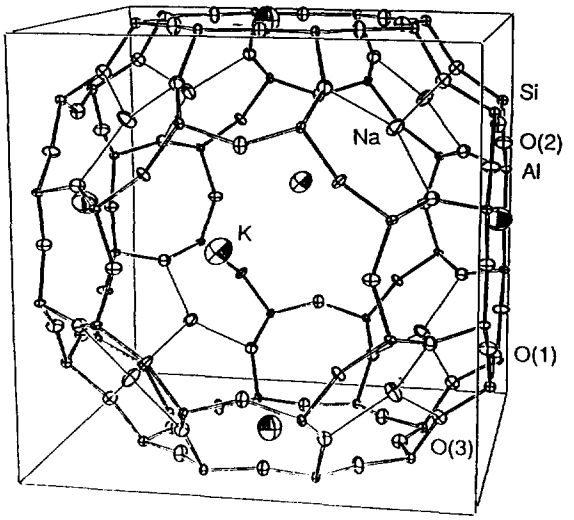

Figure 3. Large cavity of K_3Na_8H-A. See the caption to Figure 1 for other details.

O(2) oxygens in K_3-A equally contribute the coordination spheres of the 8-ring K^+ ions whereas those of O(1) oxygens in K_{12}-A are predominantly coordinated oxide anions of the K^+ ions. It is the consequences of framework distortions caused by the higher concentration of K^+ ions in large cavity of K_{12}-A.

The eight 6-rings per unit cell of both K_3-A are again fully occupied by eight Na^+ ions near their centers and the reasoning and existence of the twelfth cations, Na^+ and H^+ ions respectively for K_3Na_9-A and K_3Na_8H-A, are confirmed. Otherwise, the crystal structures of both K_3-A are nearly identical with those of Rb_3-A described above, except for some marginal differences in bond distances and angles (see Table 2 for interatomic distances and angles). Large cavity of K_3Na_8H-A is shown in Figure 3.

With those noble non-framework cationic arrangements, larger M^+ ions preferably on all larger 8-rings and the compact Na^+ ions on all 6-rings, the geometry around framework

Table 4. (Si,Al)-O-(Si,Al) Angle (deg)[a] at Framework Oxygens for Several Monopositive Cation Forms of Dehydrated Zeolite A

Zeolite A	O(1)	O(2)	O(3)
Na_{12}-A[b]	142.2(2)	164.7(2)	144.8(1)
K_3Na_8H-A	**145.0(6)**	**162.0(4)**	**143.8(4)**
K_3Na_9-A	**143.3(7)**	**161.5(4)**	**143.8(1)**
K_{12}-A[c]	128.5(6)	178.4(5)	153.7(5)
Rb_3Na_8H-A	**145.1(8)**	**159.9(5)**	**143.3(5)**
Rb_3Na_9-A	**144(1)**	**162.8(7)**	**144.4(5)**
$Rb_{11}Na$-A[d]	132.2(6)	171.8(7)	149.6(3)
Cs_3Na_8H-A[e]	145.8(6)	159.1(3)	143.5(3)
Cs_3Na_9-A[e]	145.9(8)	158.2(5)	143.3(4)
$Cs_{12.5}$-A[f]	143.8(11)	159.9(4)	145.6(8)

[a]The numbers in parentheses are the estimated standard deviations in the units of the least significant digit given for the corresponding parameters. [b]Data from reference 38. [c]Data from reference 24. [d]Data from reference 23. [e]Data from reference 21. [f]Data from reference 39.

oxide anions and (Si,Al) atoms of M_3-A are found to be remarkably relaxed ones, especially when they are compared with those of M-A with higher concentration of M^+ ions as in those of $Rb_{11}Na$-A and K_{12}-A (*vide infra*). The positions of Rb^+ ions on the 8-rings of Rb_3-A, at about 0.40 Å away from the centers, and the closer approaches of Rb^+ and K^+ ions to the framework in Rb_3-A and K_3-A, respectively, are the consequences of this remarkable undistortion found in M_3-A. In cases of $Rb_{11}Na$-A and K_{12}-A with the high concentration of large M^+ ions per unit cell, it seems apparent that the oxide anions modify their positions simultaneously toward the M^+ ions on the 8-rings as well as those located deep in large cavity in order to accommodate the electrons of the anions within the primary coordination spheres of M^+ ions. This results in the locations of Rb^+ ions at the centers and some oxide anions further away from the M^+ ions on the 8-rings of $Rb_{11}Na$-A and K_{12}-A.

The effects of these remarkable relexation of framework atoms in M_3-A can be seen in the bond angles of (Si,Al)-O(i)-(Si,Al), $i=1$ to 3, as summarized in Table 4. For example, the bond angles of (Si,Al)-O(3)-(Si,Al) are 145.5(10) and 143.3(5)°, respectively for Na_{12}-A[38] and Rb_3Na_8H-A, while that in $Rb_{11}Na$-A is 149.6(3)°. This effect is even more profound in the cases of those in 8-rings, (Si,Al)-O(1)-(Si,Al) and (Si,Al)-O(2)-(Si,Al), *i.e.* 145.1(8) and 159.9(5)° for Rb_3Na_8H-A and 132.2(6) and 171.8(7)° for $Rb_{11}Na$-A, respectively. Larger differences in those bond angles are noticed in the cases of K_3-A and K_{12}-A, while rather small changes are seen in those of Cs_3-A[21,22] and $Cs_{12.5}$-A[39] (see Table 4). The changes in these bond angles of K_{12}-A and $Rb_{11}Na$-A indicate that oxide anions at O(1) of the 8-rings further recess toward the centers of 8-rings than those in M_3-A. The structural strains caused by these distortions on O(1) oxide anions seem to be accommodated by simultaneous modification of positions at O(2) anions, away from the center of the 8-ring, resulting in the remarkable distortions of the 8-rings and the reduction of window sizes with probably less favorable sorption properties.

However, M_3-A with the noble arrangement of cations. as mentioned above, turned out to have remarkably undistorted framework atoms of 8-rings, the main windows for the passage of gas molecules, as seen in its original forms of Na-A. It is to achieve these undistorted and unreduced noble 8-ring-windows with the maximized effective volume of cavities that M_3-A zeolites have been selected as one of the efficient zeolite A systems for gas encapsulation.

Acknowledgment. This work was supported by MOTIE (Ministry of Trade, Industry, and Energy) of Korea and by COSMO Industrial Co., Ltd.

References

1. Breck, D. W. *Zeolite Molecular Sieves: Structure, Chemistry, and Uses*; John Wiley & Sons: New York, 1974, p 623.
2. Fraenkel, D. *Chem. Tech.* **1981**, *1*, 60.
3. Barrer, R. M.; Vaughan, D. E. W. *Trans. Faraday Soc.* **1971**, *67*, 2129.
4. Vansant, E. F. *Innovation in Zeolite Material Science*; Grobet, P. J. *et al.* Eds., Elsevier Science Publishers: Amsterdam, 1980, pp 143.
5. Barrer, R. M.; Vaughan, D. E. W. *Surface Science* **1969**, *14*, 77.
6. Cook, G. A. *Argon, Helium, and the Rare Gases*; Interscience: New York, Vol. 1, 1961, p 228.
7. Barrer, R. M.; Vaughan, D. E. W. *J. Phys. Chem. Solids* **1971**, *32*, 731.
8. Barrer, R. M.; Vaughan, D. E. W. *Trans. Faraday Soc.* **1967**, *63*, 2275.
9. Barrer, R. M.; Gibbons, R. M. *ibid*, **1963**, *59*, 2569.
10. Barrer, R. M.; Gibbons, R. M. *ibid*, **1965**, *61*, 948.
11. Fraenkel, D.; Shabtai, J. *J. Am. Chem. Soc.* **1977**, *99*, 7074.
12. Fraenkel, D. *J. Chem. Soc. Faraday Trans. I* **1981**, *77*, 2029.
13. Fraenkel, D.; Ittah, B.; Levy, M. *J. Chem. Soc., Chem. Commun.* **1984**, 1391.
14. Yoon, J. H.; Heo, N. H. *J. Phys. Chem.* **1992**, *96*, 4997.
15. Heo, N. H.; Rho, B. R.; Kim, D. H.; Kim, J. T. *Hwahak Konghak* **1991**, *29*, 407.
16. Kim, D. H.; Heo, N. H.; Kim, J. T. *ibid*, **1991**, *29*, 717.
17. Kwon, J. H.; Cho, K. H.; Kim, H. W.; Suh, S. H.; Heo, N. H. *Bull. Kor. Chem. Soc.* **1993**, *14*, 583.
18. Kwon, J. H., ME Thesis, Kyungpook National University, 1993.
19. Kim, D. H.; Heo, N. H.; Kim, J. T. *Hwahak Konghak* **1994**, *32*, 281.
20. The nomenclature refers to the contents of the $Pm\bar{3}m$ unit cell: e.g., Na_{12}-A represents $Na_{12}Si_{12}Al_{12}O_{48}$, and Rb_3Na_8H-A represents $Rb_3Na_8HSi_{12}Al_{12}O_{48}$.
21. Cho, K. H.; Kwon, J. H.; Kim, H. W.; Park, C. S.; Heo, N. H. *Bull. Kor. Chem. Soc.* **1994**, *15*, 297.
22. Heo, N. H.; Cho, K. H.; Kim, J. T.; Seff, K. *J. Phys. Chem.* **1994**, *98*, 13328.
23. Firror, R. L.; Seff, K. *J. Am. Chem. Soc.* **1977**, *99*, 1112.
24. Leung P. C. W.; Kunz, K. B.; Maxwell, I. E.; Seff, K. *J. Phys. Chem.* **1975**, *79*, 2157.
25. Handbook of Chemistry and Physics; Chemical Rubber

Co., Cleveland, OH 64th ed., 1983, p F-187.
26. Shannon, R. D.; Prewitt, C. T. *Acta Cryst.* **1969**, *B25*, 925.
27. Jeong, H. K.; Kim, J. S.; No, K. T. The Proceedings of 72nd Annual Meeting of Korean Chemical Society, 1993, p 80.
28. Charnell, J. F. *J. Crystal Growth* **1971**, *8*, 291.
29. Cruz, W. V.; Leung, P. C. W.; Seff, K. *J. Am. Chem. Soc.* **1978**, *100*, 6997.
30. Mellum, M. D., Seff, K. *J. Phys. Chem.* **1984**, *88*, 3560.
31. International Tables for X-ray Crystallography, Kynoch Press, Birmingham, England, 1974, Vol. IV, pp 61-66.
32. Calculations were preformed with *Structure Determination System, MolEN*, Enraf-Nonius, Netherlands, 1990.
33. Blackwell, C. S.; Pluth, J. J.; Smith, J. V. *J. Phys. Chem.* **1985**, *89*, 4420.
34. Doyle, P. A.; Turner, P. S. *Acta Crystallogr., Sect. A*, **1968**, *24*, 390.
35. Reference 31, pp 73.
36. Cromer, D. T. *Acta Crystallogr.* **1965**, *18*, 17.
37. Reference 31, pp 149-150.
38. Yanagida, R. Y.; Amaro, A. A.; Seff, K. *J. Phys. Chem.* **1973**, *77*, 805.
39. Heo, N. H.; Seff, K. *J. Am. Chem. Soc.* **1987**, *109*, 7986.

Theoretical Study of Bonding and Electrical Conductivity in the Ternary Molybdenum Oxide KMo_4O_6

Dae-Bok Kang

Department of Chemistry, Kyungsung University, Pusan 608-736, Korea
Received June 7, 1995

The electronic band structure and electrical properties of KMo_4O_6 containing chains of condensed molybdenum octahedra are analyzed by means of the extended Hückel tight-binding method. KMo_4O_6 has partially filled bands of 1D as well as 3D character. They also exhibit the anisotropic band dispersions with bandwidths much larger along the c^* axis than along the directions perpendicular to it. Thus, conduction electrons are essentially delocalized along the c^* direction (*i.e.*, the chain of condensed molybdenum octahedra) in the solid. The 1D band of two partially filled d-block bands leads to Fermi surface nesting with the wave vector $\mathbf{q} \cong 0.3c^*$. The CDW instability due to this nesting is expected to cause the phase transition associated with the resistivity anomaly at low temperature. The characteristics of metallic behavior in the crystallographic ab plane are explained on the basis of the unnested 2D Fermi surfaces.

Introduction

Recently, Greenblatt *et al.*[1] prepared single crystals of KMo_4O_6 by electrolysis of a mixture of K_2MoO_4 and MoO_3. Their X-ray diffraction analysis shows that the structure of the compound is similar to that of $NaMo_4O_6$ prepared by Torardi and McCarley,[2] which contains chains of trans-edge-sharing Mo_6 octahedra. Also, the electrical resistivity and magnetic susceptibility measurements on crystal samples[1] show that KMo_4O_6 is metallic along the direction of the chains of Mo octahedra down to 100 K, below which it undergoes a metal-insulator phase transition, while KMo_4O_6 remains metallic along the direction perpendicular to these chains down to 2 K with no transition to semiconducting behavior. The conductivity of the latter case is found to be much lower than that of the former. This suggests that the electronic properties of KMo_4O_6 should be highly anisotropic.

In the present work, we have undertaken the electronic band structure calculations of KMo_4O_6 on the basis of the extended Hückel tight-binding (EHTB) method[3] and analyzed the nature of its partially filled bands to examine the anisotropy of the electronic conductivity described above and the problem of whether a resistivity anomaly at low temperature is associated with a charge density wave (CDW) instability. The atomic parameters used in our calculations are summarized in Table 1.

Crystal Structure

Previous to a discussion of the electronic band structure of KMo_4O_6, it is necessary to describe the essential features of its crystal structure. KMo_4O_6 is made up of two Mo_4O_4 chains of trans-edge-sharing Mo_6 octahedra per unit cell which are linked by trigonally bonded oxygen atoms. K^+ ions reside in approximately cubic coordination in the channels between the cross-linked chains. The structure of this compound is tetragonal (space group $P\bar{4}$).[1] A projection view of the resulting structure along the c axis is shown in Figure 1. The Mo_6O_{16} cluster in KMo_4O_6 is also shown in Figure 2, with the main interatomic distances collected in Table 2.

In an alternative description, the trans-edge-sharing Mo chains of this molybdate may be considered as constructed from two kinds of inoganic fragments, apical MoO_5 and basal MoO_4 (for the purpose of clarity, the Mo-O bonds of each fragment are represented by a thick line.) as shown in Figure